Australian Journal of Basic and Applied Sciences, 1(4): 678-686, 2007
ISSN 1991-8178

Global Ionospheric Response to the Magnetic Storm of 21 October 1999

A. Mahrous

Helwan University, Faculty of Science, Physics Dept., Cairo, Egypt.

Abstract: The present work aims to investigate the 21 October 1999 magnetic storm and its global ionosphere-magnetosphere response. The study uses a combination of ionosonde and magnetometers data; in addition, the data from satellite in-situ measurements, such as the Defense Metrological Satellite Program (DMSP), TOPographic EXplorer (TOPEX) and WIND. A new analytical method has been used to analyze the ¦oF2 ionospheric data from eleven ionosonde stations. According to that analytical method, the ¦oF2 data has been normalized to a central location, and local time correction (LTC) values have been calculated for each station. The integrated LTC data from all stations from both eastern and western hemispheres showed a global response to the magnetic storm, which is synchronized with the storm main phase manifested by the sudden decrease in D_{st}. During the main phase of the storm, the D_{st} index showed a large fall with a minimum value of –240 nT. The interplanetary Bz reversed polarity in a 19 nT southward excursion that led to detection of a prompt penetration electric field. The auroral electrojet index AE was used as indicator of high latitude convection effects on the ionospheric electric fields through prompt penetration. The global relative deviation D¦oF2 showed a damping of about -55% during the main negative phase of that ionospheric storm; moreover, the positive phase occurred before the negative one, in harmony with the results of previous studies. We observed a similarity in the behavior of both D¦oF2 and the vertical E ´ B drift during the storm. On the other hand, the DMSP results showed a disturbance in the plasma drift velocity, while TOPEX showed asymmetrical equatorial anomaly of the global TEC.

Key words:

INTRODUCTION

Electric fields, thermospheric meridional winds, a composition bulge and high latitude particle precipitation have been suggested as probable physical mechanisms to explain the ionospheric reaction to geomagnetic storms observed at different latitudes (Fuller-Rowell *et al*., 1994; Prölss, 1995; Danilov, 2001; Mansilla, 2004, and references therein). During the geomagnetic disturbance there is an input of energy into the polar ionosphere, which changes several thermospheric parameters, such as composition, temperature and circulation. Composition changes directly influence the electron concentration in the F2 region, while circulation spreads the heated gas to lower latitudes. The conflict between the storm-induced circulation and regular one determines the spatial distribution of the negative and positive phases. There are still unsolved problems (Danilov, 2001), the most acute ones are: the appearance of positive phases before the beginning of the geomagnetic disturbance, the occurrence of strong negative phases at the equator, the role of vibrationally excited nitrogen in forming negative phase, and the relation of positive phases to the dayside cusp.

A possible cause for the negative storm effect at low latitudes would be the arrival of the neutral winds carrying the composition changes. This is supported by satellite measurements obtained during the first part of the recovery phase of the intense geomagnetic storm at the crest region (Mansilla, 2003).

During geomagnetic storms, the disturbed solar wind compresses the Earth's magnetosphere, and intense electric fields occur that are mapped along geomagnetic field lines to the high-latitude ionosphere (Jakowski *et al*., 1999; Yizengaw *et al*., 2004). Energetic particles precipitate to the lower thermosphere and below, expanding the auroral zone and increasing significantly the ionospheric ionization at higher latitudes (Yizengaw *et al*., 2005).

Intense electric currents couple the high latitude ionosphere to the magnetosphere, and the enhanced energy input causes considerable heating of the ionized and neutral gases. This leads to uneven expansion of the thermosphere producing pressure gradients, which drive strong neutral winds (Buonsanto, 1999). The disturbed neutral winds produce polarization electric fields by a dynamo effect (Aarons and Rodger, 1991) as they collide

Corresponding Author: A. Mahrous, Helwan University, Faculty of Science, Physics Dept., Cairo, Egypt.
Email: amahrous@helwan.edu.eg

with the plasma in the presence of the Earth's magnetic field (Blagoveshchensky *et al*., 2003). These electric fields in turn further affect the neutrals and the plasma, illustrating that the ionized and neutral species in the upper atmosphere are closely coupled.

The horizontal component of the geomagnetic field at the magnetic dip equator reflects the change in the equatorial plasma fountain, and the difference between H at the equator and at a non-equatorial location is a good indicator of the vertical E ´ B drift (Horvath and Essex, 2003). Moreover, the enhanced downward E ´ B drift is the cause of such nighttime enhancement due to plasmasphere compression (Foster *et al*., 2002).

In our study, we aim to provide a contribution to the understanding of such effects during the occurrence of a high-intensity and long duration magnetic storm on 21 October 1999.

Magnetospheric Response:

A strong magnetic storm was recorded on 21 October 1999 due to the passage of a coronal mass ejection detected by SOHO/LASCO on 18 October (Dal Lago *et al*., 2006). Its impact on the Earth's magnetosphere appeared about two days later. Fig. 1 shows the D_{st} index (top panel), IMF Bz component measured by WIND (middle panel) and the auroral electrojet index AE (bottom panel).

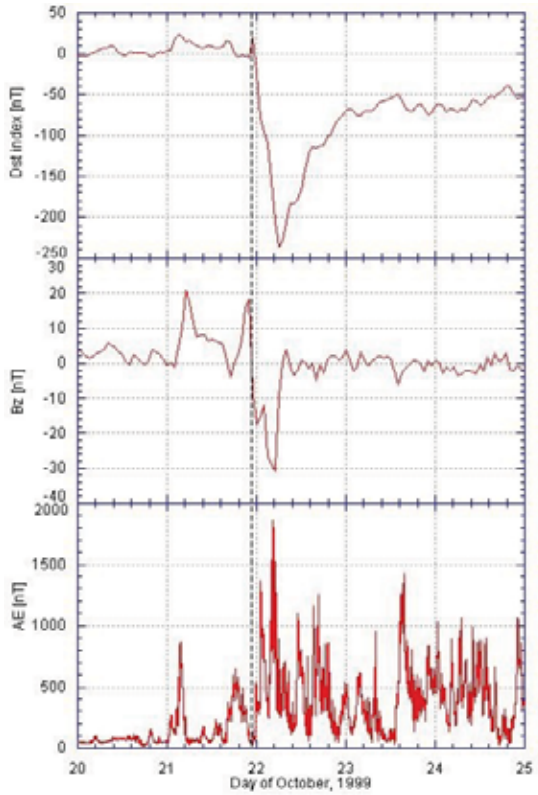

Fig.1: Dst index (top panel), IMF Bz component measured by WIND (middle panel) and the auroral electrojet index AE (bottom panel). The vertical dashed line represents the triggering time of the SSC main phase.

This storm occurred in only one step decrease after the Sudden Storm Commencement (SSC) at 22UT on October 21st, defined by a vertical dashed line in the figure, with a minimum value of the D_{st} index of –240 nT when the Bz reversed polarity in a 19 nT southward excursion.

The AE index intensity remained quite high during the storm period. The sudden northward Bz intensity variation (that is, a decrease in southward Bz) occurred on 21st at 22UT and a simultaneous sudden decrease in the AE index are consistent with the hypothesis of the penetration of an eastward disturbance electric field (Fejer, 1991; Sobral *et al*., 1997).

Ionosonde Data:

Ground-based hourly ¦oF2 data, which is proportional to the square root of NmF2, provided by the Space Physics Interactive Data Resource (SPIDR) of the NGDC-NOAA have been collected during the time period 20~25 October 1999. The station codes, names and their geographical longitudes and latitudes are listed in Table 1. The locations of the eleven-ionosonde stations used in this study are shown in Fig. 2. The circles represent the stations location, and the lines represent the grid to the central station.

Table 1: A list of ionospheric stations from which data were used in this study with their geographical longitude and latitude,* Central station

Code	Station	Long.	Latit.
S1	Leningrad	30.7	60
S2	Juliusruh*	13.4	54.6
S3	Chilton	-1.3	51.6
S4	Moscow	37.3	55.5
S5	Uppsala	17.6	59.8
S5	Millstone	-71.5	42.6
S7	Boulder	-105.3	40
S8	Novosibirsk	83.2	54.6
S9	Hobart	147.3	-42.9
S10	Grahamstown	26.5	-33.3
S11	Port-Stanley	-57.9	-51.7

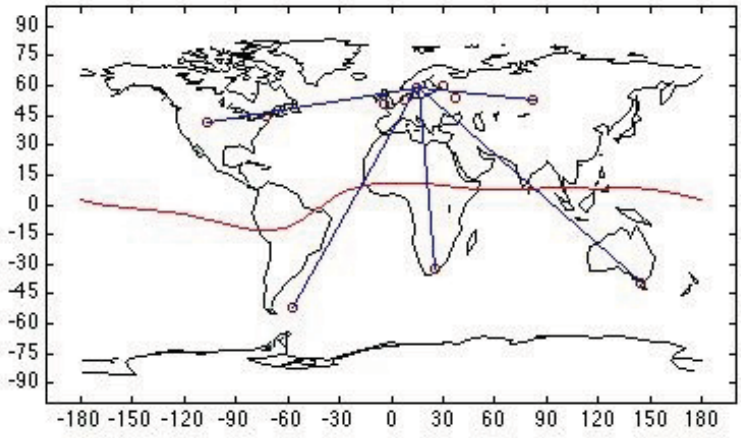

Fig. 2: Geographic map of the eleven ionosonde stations (circles) that provided data for this study, with normalization to the central station as the intersection of the (lines).

A new more general method has been used to analyze the data from the above stations (Mahrous & Radicella, 2006). Calculating the average value of the geographical longitude of the 11 stations, it was equal 10.9 degree. We define the central station among all the triggered stations; this should be the nearest one to the average. Upon this simple calculation, Juliusruh station was the central station. Calculating the local time difference between each station and the central one, that local time correction (LTC) should be added (or subtracted) to the original data. It should be noted also that the same results should be obtained in case of choosing any other station and calculating the LTC corresponding to it.

Fig.3 shows the diurnal variation of ¦oF2 critical frequency in MHz normalized to the central station during 20~25 October 1999. Station names are written on the y-axis, the vertical dashed line represents the triggering time of the SSC. The last three stations of Fig.3, which are S9, S10, S11, belong to the southern hemisphere while the rest belong to northern hemisphere. It is interesting to notice that all the 11 stations having the same behavior, that is, a regular daily variation within the frequency range (3.5~11 MHz) on undisturbed day of 20th, and a damping by the end of 21st at 22UT which is synchronized with the storm main phase. The decrease in the ¦oF2 continued for the whole disturbed day of 22nd, reaching a maximum value of 2 MHz for stations (S1, S2, S3, S5, S8, S9). The recovery phase started on the 23rd by the return of ¦oF2 to the regular values.

Global Ionospheric Response:

According to the used analytical method, the ¦oF2 data has been normalized to a central location, therefore, it is possible to draw all the data from the 11 stations in one figure like the dot-points in Fig.4.

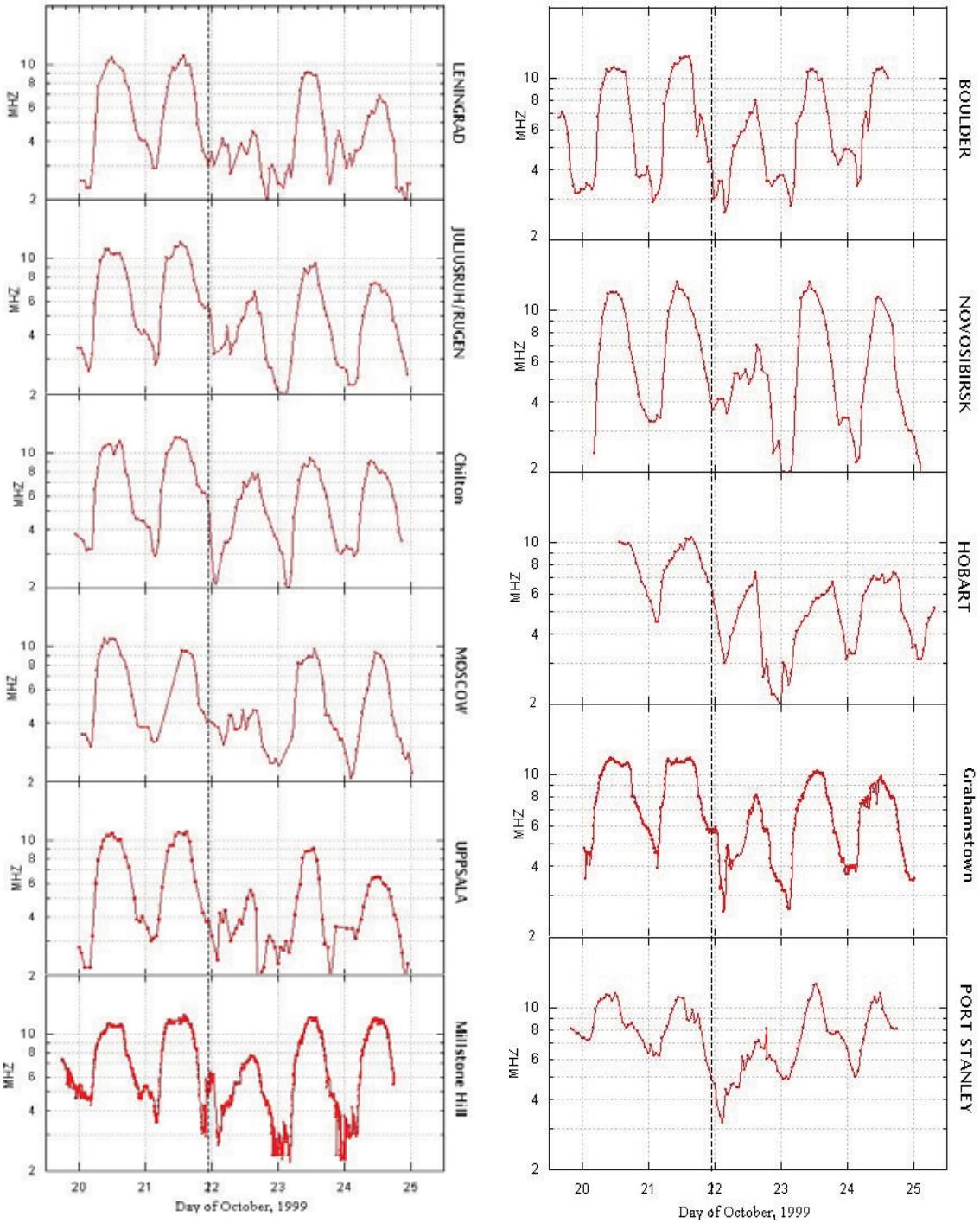

Fig. 3: Diurnal variation of ¦oF2 parameter with LTC during 20~25 October, 1999. Station names are written on the y-axis, the vertical dashed line represents triggering time of the SSC.

The average value of the whole data is represented by the curve in the same figure. The figure also shows a regular diurnal variation of ¦oF2 value during 20th and 21st, a damping during 22nd and recovery by 23rd. The signature of the geomagnetic storm on the global ionospheric response manifested by the ¦oF2 parameter is clearly shown in that figure.

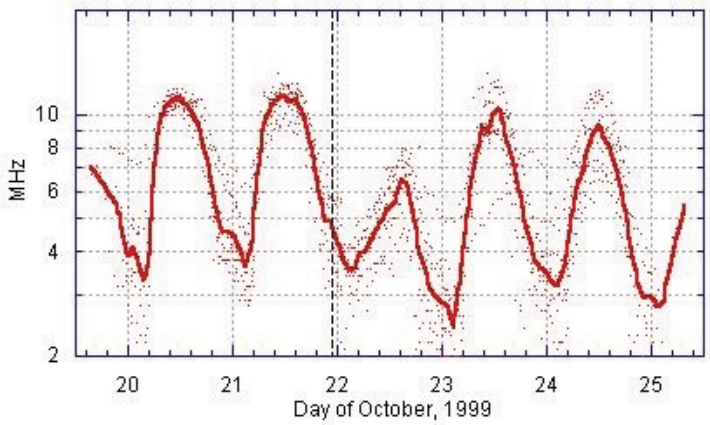

Fig. 4: The mean value of ¦oF2 measured by the 11 stations, the vertical dashed line represents triggering time of the storm main phase.

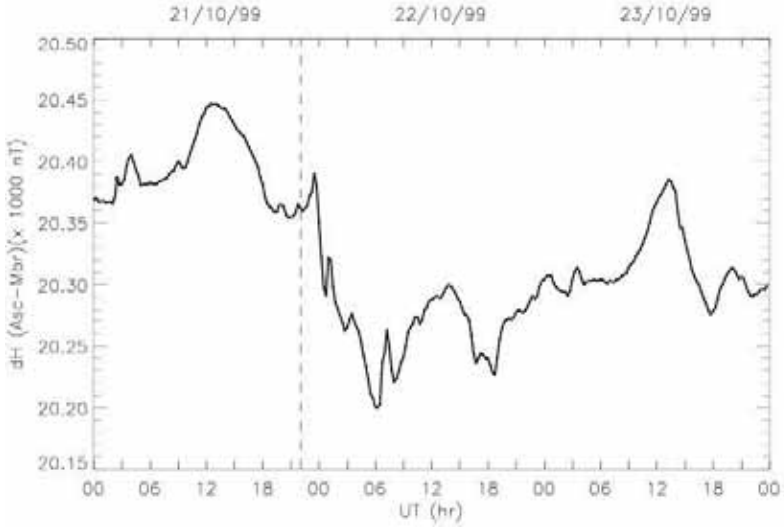

Fig. 5: The relative deviation of ¦oF2 measured by the 11 stations, the vertical dashed line represents triggering time of the storm main phase.

As an index of the ionospheric disturbance, we calculated the relative deviation of critical frequencies from the quiet level D¦oF2. This technique has been used by many authors like Blagoveshchensky *et al*.(2003) and Danilov A.D. (2001), according to the following equation

$$D¦oF2 = (¦_{dis} - ¦_{qui})/ ¦_{qui} \times 100\% \quad (1)$$

Where $¦_{dis}$, $¦_{qui}$ are the critical frequency of F2 layer during disturbed and quite periods respectively. Fig.5 shows the relative deviation of ¦oF2 measured by the 11 stations, the vertical dashed line as represented in the previous figures.

Significant negative low amplitude deviation of D¦oF2 is observed in connection with the SSC, reaching its maximum value -55% on 22nd at 09UT. The positive enhancement of D¦oF2 appeared two times. The first peak started on 20th at 20UT, having the maximum of 30% on 21st at 00UT and recovery within 3 hours. The second peak occurred on 21st at 22UT with maximum deviation of 30%, coincident with the SSC onset.

Vertical E ´ B drift:

The equatorial electrojet current produces the strong enhancement of the H-component magnetic field, which is observed by magnetometers located near the magnetic equator. The D_{st} ring current and global dynamo contribution to the H-component can be removed by subtracting the H-component recorded at a non-equator magnetometer ($H_{non-equator}$) from the H-component value measured by a magnetometer at the magnetic equator ($H_{equator}$). The difference is the only part of the H-component field that is related to the equatorial electrojet current contribution which, in turn, is directly related to the east-west electric field that triggered the system to create the electrojet current. Therefore, the E × B drift can be estimated using the resulting DH ($H_{equator} - H_{non-equator}$) value of the H-component field (Yizengaw *et al*., 2005).

Figure 6 displays the parameter DH for the two stations Ascension Island (Asc) at (-7.9° N, 345.62° E geomagnetic) and M' Bour (Mbr) at (14.39° N, 343.04 E geomagnetic), which have been used to determine $H_{equator}$ and $H_{non-equator}$, respectively. The figure also shows a damping of DH of about –1.8 nT occurred on October 21 at 23 UT.

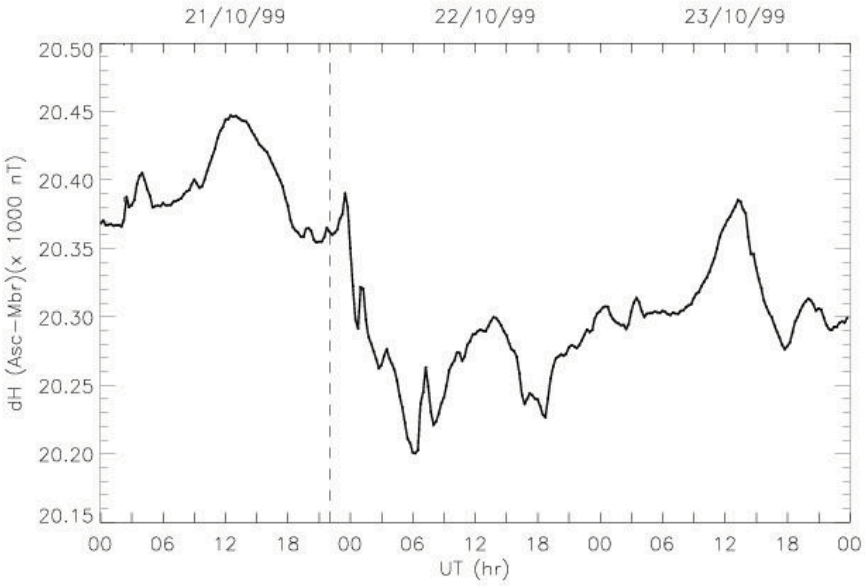

Fig. 6: The DH (difference between the horizontal component of the geomagnetic field (H) at the equator and at non-equator regions) obtained from the magnetometer data at Ascension Island (Asc) at (-7.9° N, 345.62° E geomagnetic) and M'Bour (Mbr) at (14.39° N, 343.04 E geomagnetic) to estimate vertical E ´ B drift.

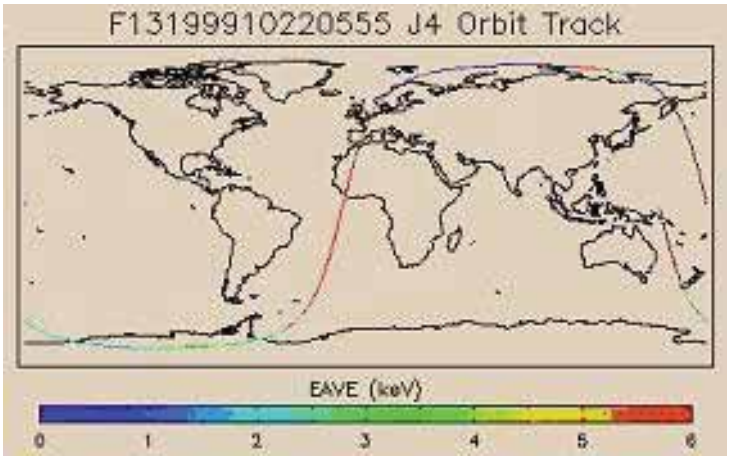

Fig. 7: The ground orbit track of DMSP F13

DMSP Data:

The DMSP satellites circle the Earth in Sun-synchronous dawn-dusk orbits at nearly 850 km altitude. The DMSP F13 flew close to the central ionosonde station, as shown in Fig. 7, at 6:30 UT. The data of DMSP F13 during October 22 is shown in Fig. 8. The top panel shows the plasma temperature observed at the satellite height for both ions (continues line) and electrons (points). The second, third and fourth panels, from the top, represent the plasma drift velocities in x, y and z directions; and the bottom panel indicates the ion and electron fluxes. The figure shows that the maximum flux density of 2×10^5 ions cm^{-3} take place within the mid-latitude (between 60° – 1.2° S geographic) region. The plasma temperature depict a variation between 1500 k ~ 5000 k for both ions and electrons over the same region.

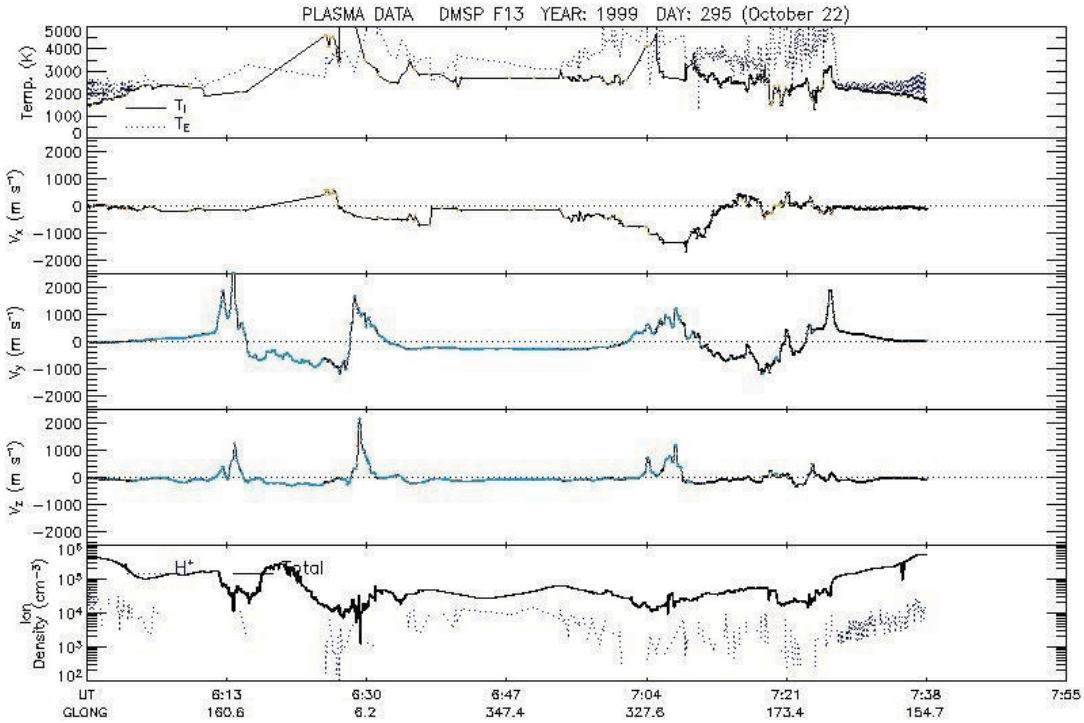

Fig. 8: The topside F-region plasma temperature (top), plasma drift velocities in x, y and z directions (2^{nd}, 3^{rd} and 4^{th} panel from top), and ions and electron flux (bottom) obtained from the DMSP F13 satellite during October 22.

Topex Data:

Traveling in a 66-deg inclination orbit at an altitude of 1336 km, the TOPEX satellite provides about 95% of full geographic coverage of the Earth's oceans approximately every 10 days. TOPEX uses a dual-frequency altimeter to measure the range delay difference between the two frequencies and to compute the ionospheric range error, and thus obtains downward viewing TEC information. The TOPEX altimeter measures the vertical electron content beneath the satellite. Since the TOPEX altimeter is designed only to measure ocean heights, there are data gaps over landmasses as shown in the tracks of Fig.9. The colours of the tracks are corresponding to the density of the vertical electron content beneath the satellite during October 21^{st}. The figure shows asymmetrical equatorial anomaly of the global TEC.

RESULTS AND DISCUSSIONS

The case study of the ionospheric response to the magnetic storm of 21 October 1999 has revealed many interesting features. The SSC occurred on October 21^{st} at 22UT as a result of southward turning of IMF Bz, after which the D_{st} index reached its minimum value of –240 nT.

The simultaneous sudden decrease in the AE index synchronized with the sudden southward Bz intensity variation occurred on 21^{st} at 22UT was the signature of the penetration of an eastward disturbance electric field.

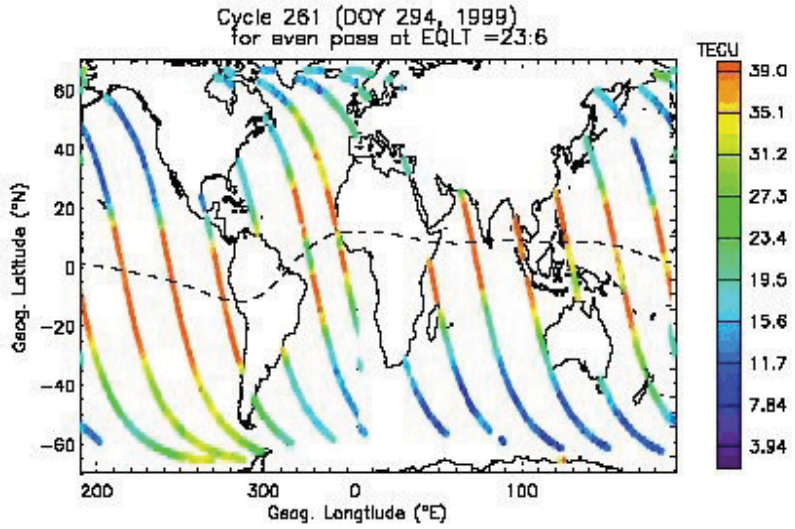

Fig. 9: TOPEX ground tracks identified by a colour code corresponding to the total electron content.

We used a new more general method to analyze the data form the 11 stations used in this study. According to that analytical method, the ¦oF2 data has been normalized to a central location. It was interesting that all the stations distributed in both northern and southern hemispheres having the same ¦oF2 trend during the storm (Fig. 3), which allowed us to study the global ionospheric response of such magnetic storm. A regular daily variation of ¦oF2 within the frequency range 3.5~11 MHz occurred on the undisturbed day of 20th. A damping initiated by the end of 21st at 22UT that is synchronized with the SSC.

As seen in Fig. 5, the D¦oF2 showed a significant negative low amplitude deviation observed during the storm main phase, reaching its maximum value -55% on 22nd at 09UT. This is a well-known negative ionospheric storm response. One the other hand, the positive enhancement (or peak) was also observed two times in the D¦oF2 curve.

Positive effects sometimes are being observed before the beginning of the magnetic disturbances. Some papers (Danilov and Belik, 1991, 1992; Danilov, 2001) suggests for this effect mechanism associated with soft particle precipitation in the region of the dayside cusp. Another possibility is due to the north crest movement to higher latitudes because of the storm time electric fields (Prölss, 1993).

The first maximum occurred on 21st at 00UT. We don't have an explanation of that peak except that this time is almost coincident with the arrival time of the shock associated with the ejecta from the CME, which caused the magnetic storm of our study as verified from Cane H.V. and Richardson I.G. (2003). The arrival time of that shock has been detected by ACE satellite on 21st at 02UT. This could be an explanation of the enhancement in the D¦oF2 due to the injection of the energetic particles accelerated by the shock. Further analysis is required regarding this research point.

The second peak occurred just before the beginning of the negative phase of D¦oF2. It is in harmony with the results of Danilov & Belik, (1991, 1992) and Danilov (2001) who detected such behavior during some geomagnetic storms.

The difference between the horizontal component of the geomagnetic field H at the equator and non-equator locations was used as indicator of the vertical E ´ B drift. It was interesting to notice such coincidence in the behavior of both E ´ B drift (Fig. 5) and D¦oF2 (Fig. 6) curves during the storm, which sustain the signature of the penetrating electric field during the SSC onset.

An enhancement of both fluxes and velocities of ions and electrons has been detected by DMSP F13, while, TOPEX results showed asymmetrical equatorial anomaly of the global TEC measured during the storm.

ACKNOWLEDGEMENT

Thanks are due to Prof. Radicella S. for discussing the ionosonde data, and the JPL's Physical Oceanography Distributed Active Archive Centre (PO.DAAC) for TOPEX altimeter TEC data, and NOAA Satellite and information service for DMSP SSJ4 data. The D_{st} and AE data are from WDC-2 at Kyoto University (Japan) (http://swdcdb.kugi.kyoto-u.ac.jp).

REFERENCES

Aarons, J. and A.S. Rodger, 1991. The effects of electric field and ring current energy increases on F layer irregularities at auroral and subauroral latitudes, Radio Sci., 26: 1115-1129.

Blagoveshchensky, D.V, O.M. Pirog, N.M. Polekh, L.V. Chistyakova, 2003. Mid-latitude effects of the May 15, 1997 magnetic storm. Atmos. Terr. Phys., 65: 203-210.

Buonsanto, M.J., 1999. Ionospheric storms-a review, Space Sci. Rev., 88: 563-601.

Cane, H.V., I.G. Richardson, 2003. Interplanetary coronal mass ejections in the near-Earth solar wind during 1996-2002. J. Geophys. Res., 108: 1156-1168.

Dal Lago, A., 2006. The 17–22 October (1999) solar-interplanetary-geomagnetic event: Very intense geomagnetic storm associated with a pressure balance between interplanetary coronal mass ejection and a high-speed stream. J. Geophys. Res., 111: 1029.

Danilov, A.D., 2001. F2-region response to geomagnetic disturbances. Atmos. Terr. Phys., 63: 441.

Danilov, A.D., L.D. Belik, 1992. Thermospheric composition and the positive phase of an ionospheric storm. Adv. Space Res., 12(10): 257.

Danilov, A.D., L.D. Belik, 1991. Thermospheric-ionospheric interaction during ionospheric storms Geomagnetism and Aeronomy, 31(2): 209.

Fejer, B.G., 1991. Low latitude electrodynamic plasma drifts. J. Atmos. Terr. Phys., 58: 677-693.

Foster, J.C., P.J. Erickson, A.J. Coster, J. Goldstein, and F.J. Rich, 2002. Ionospheric signatures of plasmaspheric tails, Geophys. Res. Lett., 29(13): 10.1029/2002GL015067.

Fuller-Rowell, T.J., M.V. Codrescu, R.J. Moffett, S. Quegan, 1994. Response of the thermosphere and ionosphere to geomagnetic storms. J. Geophys. Res., 99: 3893.

Horvath, I. and E.A. Essex, 2003. Vertical E×B drift velocity variations and associated low- latitude ionospheric irregularities investigated with the TOPEX and GPS satellite data, Ann. Geophys., 21: 1017-1030.

Jakowski, N., S. Schluter and E. Sardon, 1999. Total electron content of the ionosphere during the geomagnetic storm on 10 January 1997, J. Atmos. Terr. Phys., 61: 299-307.

Mahrous, A., S. Radicella, 2006. F2-Region Response to the Geomagnetic Storm of 21October 1999, proceeding of the 36th COSPAR scientific assembly, Beijing, China, 112.

Mansilla, G.A., 2004. Mid-latitude ionospheric effects of a great geomagnetic storm. Atmos. Terr. Phys., 66: 1085-1091.

Mansilla, G.A., 2003. Disturbances at F2-region heights of equatorial anomaly during geomagnetic storms. Atmos. Terr. Phys., 65: 987.

Prölss, G.W., 1995. Ionospheric F-region storms. In:Volland,H. (Ed.), Handbook of Atmospheric Electrodynamics,Vol.2.CRC Press, Boca Raton, FL, 195.

Prölss, G.W., 1993. Common origin of positive ionospheric storms at middle latitudes and the geomagnetic activity effect at low latitudes. J. Geophys. Res., 98: 5981.

Sobral, J.H., M.A. Abdu, W.D. Gonzalez, B.T. Tsurutani, I.S. Batista, Gonzalez, C. Alicia, 1997. Effects of intense storms and substorms on the equatorial Ionosphere-Thermosphere system in the American sector from ground-based and satellite data. J. Geophys. Res., 102(14): 305-14,313.

Yizengaw, E., P.L. Dyson, E.A. Essex and M.B. Moldwin, 2005. Ionosphere dynamics over the Southern Hemisphere during the 31 March 2001 severe magnetic storm using multi-instrument measurement data, Ann. Geophys., 23: 707-721.

Yizengaw, E., E.A. Essex and R. Birsa, 2004. The Southern Hemisphere and Equatorial region ionization response for September 22, 1999 severe magnetic storm, Ann. Geophys., 22: 2765-2773.